Modeling of Coal Pyrolysis Kinetics

Truls Liliedahl and Krister Sjöström
Institutionen för Kemisk Teknologi, Kungl Tekniska Högskolan, S-100 44, Stockholm, Sweden

Four different coals were instantaneously introduced into a laboratory-scale pyrolysis chamber at various temperatures, and their devolatilization profiles were analyzed with respect to kinetics. The experimental setup consisted of a gas chromatograph (GC) with a pyrolysis unit, an empty column, and a detector. Detector signals were digitalized and stored for further handling. Normally, 1,024 values were sampled at 250 Hz. For deconvolving the true instantaneous devolatilization from the observed detector response, the residence time distribution was compensated for.

An empirical model approach is developed to correlate the total devolatilization rates when instantaneously introducing a particle in a constant temperature environment. The model is also extended to pyrolysis application.

Introduction

The approaches at hand for modeling total devolatilization rates (that is, weight-loss rates) when pyrolyzing are either of a physical (kinetic) or a numerical nature. The kinetic model approaches are in some way linked to traditional reaction kinetics, while the numerical approaches are of an empirical nature and view the modeling of pyrolysis reaction kinetics more as a curve-fitting exercise.

The kinetic models may be divided into three generic categories. These are: models assuming a single reaction, models assuming a limited number of reactions in parallel, and models assuming an infinite number of reactions in parallel.

In the first kinetic approach, total devolatilization is assumed to be through a single, first-order reaction. This approach is the least complicated, but it is normally only applicable over relatively narrow temperature ranges and pyrolysis time frames.

In the second kinetic approach, devolatilization of the most important species is monitored. This approach does predict total devolatilization rates over wider temperature intervals and time frames, implying it to be more correct. One drawback with this approach is its complexity, as it calls for determination of an initial amount of volatile matter, a preexponential factor and an activation energy for each reaction included.

The third kinetic approach is an extension of the second one, as it assumes an infinite number of first-order reactions in parallel. In this approach, the initial volatile matter amounts of the reactions included are often assumed to be Gaussian with respect to the activation energy. This approach combines some of the advantages of the first two approaches discussed. It is applicable over wider temperature ranges and time frames than the first one and it is less complicated, in the sense that it calls for determination of fewer rate constants for a given accuracy, than the second one. An empirical approach, in contrast to the above discussed kinetic approaches, will be suggested in the next section and will also be used for modeling total devolatilization rates for a number of coals.

Review of Generic Approaches for Modeling Pyrolysis Devolatilization Rates

Background

For correlating, pyrolysis devolatilization rates, dm_t/dt, over time will be monitored and analyzed. A method for deriving such profiles has been described by Liliedahl et al. (1991).

Pyrolysis experiments in which particles are instantaneously introduced into a constant temperature gas phase surrounding are preferable if results are to be evaluated in the context of similar pyrolysis applications.

By correlating to devolatilization rates directly, not indirectly via devolatilization degrees, it is assumed that the numerical handling will be facilitated and the correlation quality enhanced. The reason for making this assumption is that it is the devolatilization rate, not its integral value, that in some way is proportional to a devolatilization driving force.

It is further assumed that correlation to devolatilization rates,

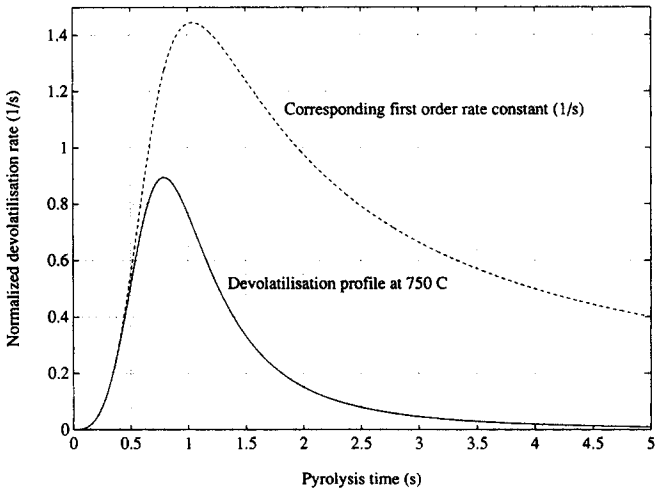

Figure 1. Normalized FID devolatilization profile for Kentucky #11 coal specimen at 750°C and corresponding first-order reaction rate constant.

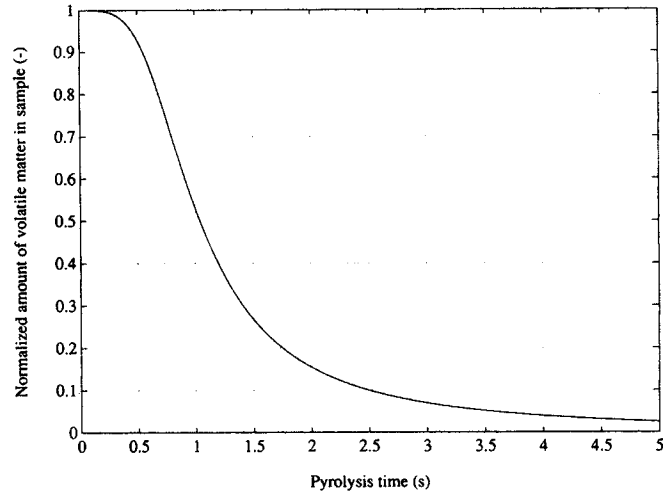

Figure 2. Normalized amount of volatile matter in sample for the Kentucky #11 coal at 750°C.

in contrast to devolatilization degrees, will more likely lead to linear devolatilization rate expressions. Correlation with respect to devolatilization degrees will also result in "slower" and "less sensitive" data, as integration is a dampening operation.

Kinetic and model approaches

Figure 1 gives the total devolatilization rate, dm_t/dt, and Figure 2 the corresponding instantaneous amount of volatile matter in the sample, m_t, for a Kentucky #11 coal specimen (see Table 1) which instantaneously was introduced into a 750°C nitrogen atmosphere. The sampling frequency was 250 Hz. As the frontside of the devolatilization profile represents the particle heatup phase only the backside of the profile can be expected to follow the isothermal kinetics to be discussed below.

The devolatilization rate constant, k, is assumed to be given by the Arrhenius expression:

$$k = k_0 \exp\left(\frac{-E}{RT_p}\right) \tag{1}$$

For the first kinetic model approach, the single first-order reaction assumption, the total devolatilization rate is assumed to follow:

$$-\frac{dm_t}{dt} = k\, m_t \tag{2}$$

With m_t being the instantaneous amount of volatile matter in the sample at time t. If m_0 denotes the initial amount of volatile matter in the sample, Eq. 2 may be rewritten:

$$-\frac{dm_t}{dt} = k\, m_0 \exp(-kt) \tag{3}$$

As the dimension of k is mass-independent, Eq. 3 may be normalized following $m'_t = m_t/m_0$ giving:

$$-\frac{dm'_t}{dt} = k \exp(-kt) \tag{4}$$

Through computation of k from experimental dm_t/dt profiles

Table 1. Coal Specimen Characteristics

Coal Specimen	SBN Code	Ultimate Analysis (%)	Promixate Analysis (% Dry)
Mine: River Queen Seam: Kentucky #11	132US40	C: 71.22, H: 4.98, N: 1.34 S: 3.28, Cl: 0.03, O-diff: 8.47	Ash: 10.68 Volatile matter: 40.66 Fixed carbon: 48.66
Mine: Powhaton Seam: Pittsburgh #8	133US42	C: 72.74, H: 4.83, N: 1.13 S: 4.41, Cl: 0.06, O-diff: 6.31	Ash: 10.52 Volatile matter: 41.77 Fixed carbon: 47.71
Mine: Westerholt	210DE34	C: 32.20, H: 1.89, N: 0.05 S: 0.96, Cl: 0.07, O-diff: 3.10	Ash: 61.23 Volatile matter: 13.05 Fixed carbon: 25.72
Mine: Crown #2 Seam: Illinois #6	511US43	C: 71.25, H: 4.51, N: 1.21 S: 4.02, Cl: 0.08, O-diff: 8.50	Ash: 10.43 Volatile matter: 42.09 Fixed carbon: 47.48

it may be concluded that k will not be constant over time, indicating this approach to be, as expected, incorrect (Figure 1). In the computations m_t was assumed to equal the cumulative sum of $-dm_t/dt$ over time subtracted from m_0. This approach is moreover only valid over relatively narrow temperature intervals, which also indicates this approach to be incorrect (Anthony et al., 1974; Howard, 1981; Solomon and Hamblen, 1983; Solomon et al., 1986). Saito et al. (1987), however, used this model successfully for correlating pyrolysis weight-loss kinetics for single coal particles (radius, 1.21–1.91 mm; weight, 10–40 mg) between 800 and 1,100°C. Nevertheless, discrete Arrhenius activation energies and frequency factors derived through this model approach tend to be apparent.

For the second kinetic model approach, the multiple single-reaction assumption, total devolatilization is assumed to occur through a number of independent reactions in parallel. Devolatilization for each reaction, i, is assumed to follow as before:

$$-\frac{dm_{it}}{dt} = k_i m_{it} \tag{5}$$

The total devolatilization rate may, if including n reactions, be written:

$$-\frac{dm_t}{dt} = \sum_{i=1}^{n} m_{i0}\, k_i \exp(-k_i t) \tag{6}$$

With the normalization criterion:

$$m_0 = \sum_{i=1}^{n} m_{i0} \tag{7}$$

The low activation energies often derived from the first kinetic model-approach discussed above may be explained by the fact that a number of first-order reactions in parallel will result in an apparent single-reaction activation energy (much) lower than the average activation energy of the participating reactions (Jüntgen and van Heek, 1970; Reuther et al., 1984). This second kinetic model approach does show, if only a sufficient number of reactions are included, good validity over time as well as temperature, implying this approach to be more correct (Jüntgen and van Heek, 1970; Jüntgen, 1984; Suuberg et al., 1978). The reliability of this approach, though, depends on the number of reactions included, resulting in the accuracy being inversely proportional to the complexity. If substituting the discrete m_{i0} values and the corresponding k_i values with a continuous function $m_0(k)$, defined for all ks, Eq. 6 may be written:

$$-\frac{dm_t}{dt} = \int_{-\infty}^{\infty} m_0(k) k \exp(-kt)\, dk \tag{8}$$

with:

$$m_0 = \int_{-\infty}^{\infty} m_0(k)\, dk \tag{9}$$

Equation 8 with 9 gives a general solution of the total devolatilization rate for this third kinetic approach. The solution will depend on the initial volatile matter distribution, $m_0(k)$. A model in which this distribution is assumed to be Gaussian with respect to the activation energy, E, around a mean activation energy, E_0, with a standard deviation, σ, has been suggested by Pitt (1962). This model has been further developed by Anthony et al. (1974), Borghi et al. (1985), and others. In this assumption is assumed for reasons of mathematical convenience that the preexponential factor, k_0, is constant implying that k only differs with respect to E. Eq. 9 may thus be written:

$$-\frac{dm_t}{dt} = m_0 \int_{-\infty}^{\infty} \frac{\exp\left[\frac{-(E-E_0)^2}{2\sigma^2}\right]}{\sigma\sqrt{2\pi}} \times k_0 \exp\left(\frac{-E}{RT_p}\right) \exp\left[-tk_0 \exp\left(\frac{-E}{RT_p}\right)\right] \tag{10}$$

With the overlaying normalization criterion:

$$1 = \int_0^{\infty} \int_{-\infty}^{\infty} \frac{\exp\left[\frac{-(E-E_0)^2}{2\sigma^2}\right]}{\sigma\sqrt{2\pi}} \times k_0 \exp\left(\frac{-E}{RT_p}\right) \exp\left[-tk_0 \exp\left(\frac{-E}{RT_p}\right)\right] dE\, dt \tag{11}$$

This expression may only be solved, as it stands, numerically. Through a nonlinear least-square fit of a number of different particle temperature devolatilization profiles, the interdependent kinetic constants E_o, k_0 and σ may be derived. This approach has successfully been used by, among others, Anthony et al. (1974), Jüntgen and van Heek (1970), and Jüntgen (1984) for correlating total devolatilization rates as well as devolatilization rates for different species. Salomon et al. (1986) used on-line FTIR analysis (TG-FTIR) for monitoring devolatilization rates of different species, and correlated the results to this approach.

Taylor-expansion of Eq. 10 around E_0 and subsequent integration from $E_0 - x$ to $E_0 + x$, with x being an arbitrary chosen parameter, gives:

$$-\frac{dm_t}{dt} \sim m_0 (q_1 + q_2 t + \ldots + q_i t^{i-1}) \exp\left[-t\, k_0 \exp\left(-\frac{E_0}{RT_p}\right)\right] \tag{12}$$

with:

$$1 = \int_0^t (q_1 + q_2 t + \ldots + q_i t^{i-1}) \exp\left[-t\, k_0 \exp\left(-\frac{E_0}{RT_p}\right)\right] dt \tag{13}$$

q_1 to q_i are temperature dependent constants also to be derived through a nonlinear least-square computation from a number of different temperature devolatilization profiles. The numer-

ical handling of Eq. 10 with Eq. 11 or Eq. 12 with Eq. 13 is not trivial due mainly to the nonlinearity of the expressions and the interdependence of the constants to be derived.

Empirical model approaches

Empirical model approaches have been suggested by, among others, Badzioch and Hawksley (1970), Kobayashi et al. (1977), and Solomon and Colkert (1979). In these approaches instantaneous amounts of volatile matter or devolatilization degrees are normally fitted to some kind of exponential expression and/or polynomial.

These approaches are often not linear in the sense that the numerical rate constants may be derived through a straight least-square computation. One reason for the nonlinearity, as discussed earlier, is that they often try to correlate instantaneous amounts of volatile matter, m_i, in contrast to devolatilization rates, dm_i/dt. This aspect is, as also discussed earlier, of importance with respect to the correlation quality. Badzioch and Hawksley (1970), for example, assume devolatilization rates during heatup to be negligible and thus do not account for the initial nonisothermal devolatilization. A brief look at Figure 1 or subsequently Figure 5, though, suggests on the contrary that 25–35% of the volatile matter is devolatilized during the initial heatup. If monitoring instantaneous amounts of volatile matter, as in Figure 2 or subsequently Figure 6, it is (much) more difficult to see this. This especially if the data sampling would be less frequent. The reason for the assumption above is thus more easily understood.

Experimental Setup and Experimental Procedure

The experimental setup is given in Figure 3 and consists of a gas chromatograph, GC, equipped with a pyrolysis unit (a Pyrojector from Scientific Glass Engineering Ltd., Victoria, Australia) as injector, an empty column, and a flame ionization detector (FID) in series. The column is empty and as short as possible, as its sole purpose is to transfer the entrained volatiles from the Pyrojector to the detector.

As the observed detector response equals the true devolatilization "smeared out" or convolved by the residence time distribution, RTD, of the apparatus, the RTD has to be compensated for. This can be achieved by Fourier transformation, inverse Fourier transformation, and subsequent filtering. For additional details see Liliedahl et al. (1991).

Four different coals were pyrolyzed at 700, 750, 800, 850, and 900°C, respectively. (The coal samples were supplied by the European Centre for Coal Specimens SBN, Eygelshoven, the Netherlands.) All samples were specially treated whole seam samples (ST-samples). ST-samples are washed at density 1.6 and sieved for 18 to 100 mesh.

The characteristics of the coals specimens studied are given in Table 1.

About a milligram of the coal sample was instantaneously injected into the Pyrojector with a solids injector. The sample will after injection rest on the quartz wool plug inside the quartz tube of the Pyrojector (Figure 3). Volatiles leaving the sample are entrained by the carrier gas (nitrogen) through the column into the detector. For data and computational han-

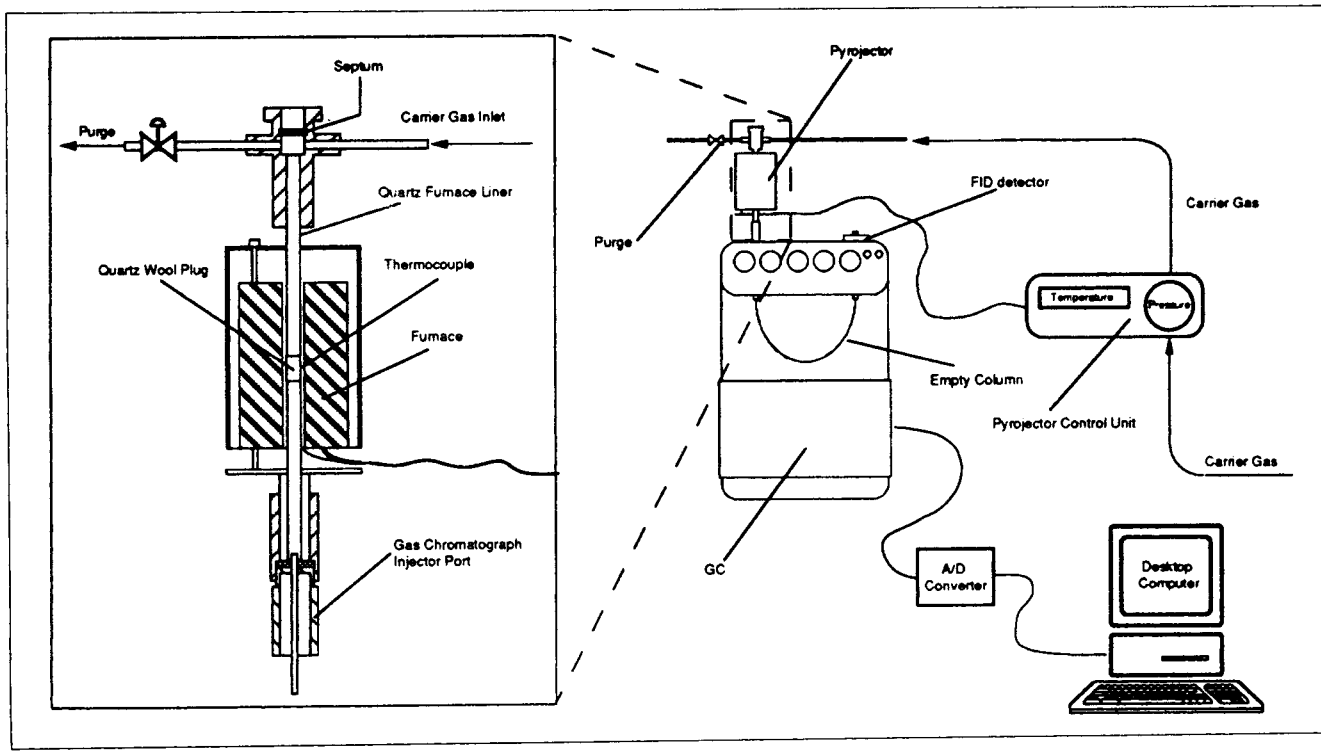

Figure 3. Experimental setup.

dling, the Matlab software with the auxiliary Signal Processing Toolbox was used (MathWorks, Inc., South Natick, MA.)

Empirical Approaches for Modeling Pyrolysis Devolatilization Rates

Assumptions and background

In the following section will be suggested empirical models for the isothermal devolatilization rate and the devolatilization rate when instantaneously introducing a solid sample into a constant temperature gas-phase surrounding.

The suggested models originate from the fact that parallel multiple-reaction kinetics is so complicated that the computation of kinetic constants tend to end up as a numerical curve-fitting exercise. For achieving acceptable accuracy over time and temperature the single-reaction models must therefore, for example, often employ "help constants." Thus often up to four kinetic constants are used. For the Gaussian distribution model approach, which normally calls for determination of the interdependent constants E_0, k_0, and σ the main disadvantages are the complexity, the nonlinearity and the fact that the model cannot be solved analytically.

If correlating devolatilization rates to numerical rather than traditional reaction kinetic expressions, the span of feasible correlation-expressions will be widened. Thus it could, for a given accuracy, be possible to predict devolatilization rates with the help of fewer rate constants and allowing for use of linear systems of equations. An additional advantage would be the possibility of including the initial nonisothermal devolatilization in the correlation-model when instantaneously introducing a particle in a pyrolysis chamber. This latter aspect is of importance when thinking in terms of pyrolysis applications.

In the suggested model approach, it is assumed that volatile matter amounts can be normalized, because a finely ground sample is made up of a large number of discrete particles and forces impacting the devolatilization kinetics are only to be expected within each particle and not between particles. Thus only the magnitude and not the shape of the devolatilization profile will be influenced by total amounts of volatile matter.

Development of empirical model

It may be concluded from the isothermal part (that is, the backside) of the devolatilization profile of Figure 1 that for the single first-order reaction assumption, k will not be constant over time. This implies that the devolatilization rate is not directly proportional to m_t.

Through simulations using the Gaussian distribution model, Eq. 10 and Eq. 11, it was concluded that devolatilization rates at given particle temperatures with acceptable accuracy may be written:

$$-\frac{dm'_t}{dt} \approx a_1 m'_t + a_2 m'^3_t \qquad (14)$$

Figure 4 shows a simulation in which Eq. 10 with Eq. 11 is approximated by Eq. 14 in a least-squares sense at two different temperatures. As seen the two curves are almost on top of each other.

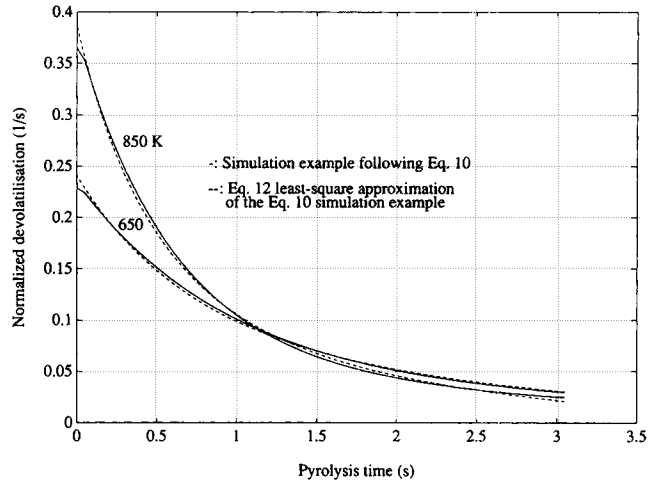

Figure 4. Example where Eq. 10 devolatilization simulation is fitted to Eq. 14 in least-square sense at two temperatures.

In accordance with Eq. 14, the total devolatilization reaction will initially be of an apparent third-order, that over time asymptotically will approach an apparent first-order. By comparing simulations at different particle temperatures it was further concluded that Eq. 14, with respect to the temperature approximately may be written:

$$-\frac{dm'_t}{dt} \approx (a'_1 m'_t + a'_2 m'^3_t)\exp(b\,T_p) \qquad (15)$$

a'_1, a'_2, and b are rate constants assumed to be specific for a given coal specimen. This expression could thus be used for predicting constant particle temperature devolatilization rates with the advantage of being much less complicated than the Eq. 10 with the Eq. 11 expression which it approximates.

Equation 15 though, only accounts for the isothermal part (that is, the backside) of the devolatilization profile. For the nonisothermal part (that is, the frontside) of the devolatilization profile, the devolatilization will be heat-transfer constrained. After having intantaneously introduced a particle into a constant temperature gas phase surrounding, the particle temperature will initially increase rapidly, but over time asymptotically approach the gas phase temperature, T_{gas}.

The rate at which the particle temperature increases, dT_p/dt, may be assumed to be proportional to the difference between the gas phase and the particle temperatures by a constant, given by $h/\rho_p C_p r_{eff}$. Thus, the intraparticle gradients are assumed to be negligible (Nilsson, 1991; Pyle and Zaror, 1984). Solution of this assumption gives:

$$T_p = T_{gas} - (T_{gas} - T_0)\exp\left(\frac{-h}{\rho_p C_p r_{eff}}\,t\right) \qquad (16)$$

Equations 15 and 16 therefore, give the normalized total devolatilization rate if instantaneously introducing a finely ground sample into a constant temperature gas-phase surrounding.

Equations 15 and 16 have a few drawbacks, though. One is its nonlinearity and another is that it cannot be solved ana-

lytically. These drawbacks may be bypassed if approximating Eqs. 15 and 16 as:

$$-\frac{dm'_t}{dt} \sim a \exp(b\ T_{gas}) c\, t^3\, m'^{\,3}_t \qquad (17)$$

This expression is empirical and results from a correlation of a number of different pyrojector temperature devolatilization profiles.

In Eq. 17, a and b are numerical rate constants assumed to be specific for a given coal, and c is a correlation factor between 0 and 1. It is introduced to compensate for the error introduced by excluding intraparticle temperature gradients. For quantifying these gradients the Biot number (hr_{eff}/K) may be used. c will thus approach 1 for small Biot numbers and asymptotically approach 0 for large Biot numbers. For the coal samples studied, it is assumed that $c \approx 1$, as the samples were finely ground. This assumption is based on the conclusions made by Badzioch and Hawksley (1970), Nilsson (1991), Pyle and Zaror (1984), and Agarwal et al. (1984), indicating devolatilization to be externally heat-transfer controlled for particles with $r_{eff} < 1$ mm.

With $c = 1$, Eq. 17 becomes:

$$-\frac{dm'_t}{dt} \sim a \exp(b\ T_{gas}) t^3 m'^{\,3}_t \qquad (18)$$

a and b may be derived through a straight least-square fit from a number of different gas temperature devolatilization profiles.

Solution of Eq. 18 gives the normalized instantaneous amount of volatile matter as:

$$m'_t = \sqrt{\frac{2}{a \exp(b\ T_{gas}) t^4 + 2}} \qquad (19)$$

Insertion of Eq. 19 into Eq. 18 gives the normalized total devolatilization rate as:

$$-\frac{dm'_t}{dt} = a \exp(b\ T_{gas}) \left[\frac{2t^2}{a \exp(b\ T_{gas}) t^4 + 2}\right]^{1.5} \qquad (20)$$

Equation 20 gives the normalized total devolatilization rate as a function of pyrolysis time and gas temperature. If seeking absolute values, the normalized amounts or the normalized rates are to be multiplied by the initial volatile matter amount, m_0.

It should be noted that not only devolatilization rates of the hydrocarbons (FID detectables) may be studied, but in addition, for example, the sulfur compounds (FPD detectables) or the nitrogen compounds (NPD detectables) may be studied.

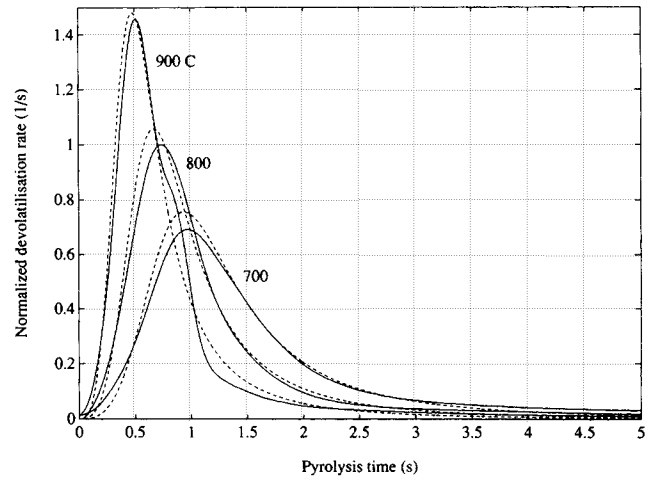

Figure 5. Experimental and computed normalized devolatilization profiles for the Kentucky #11 coal specimen at 700, 800 and 900°C.

Results

The experimentally derived rate constants, a and b for the FID detectables are given in Table 2.

The quality of the suggested model-approach is exemplified in Figure 5. This figure gives the experimental and from Eq. 15, the computed normalized total devolatilization profiles for the Kentucky #11 coal specimen, using the constants in Table 2 at 700, 800, and 900°C. In Figure 5 it may be seen that the suggested model approach predicts total devolatilization rates over the time frames and temperature intervals studied with acceptable accuracy. This conclusion was also found to be true for the other coals specimens studied.

Figure 6 provides the experimental and from Eq. 18 provides computed normalized instantaneous amount of volatile matter for the example in Figure 5.

Applications of Suggested Model

The suggested model approach can be applied within process and rector design.

Following Eq. 19 the devolatilization degree, X_{th}, can in a continuous pyrolysis reactor with the solid-phase holdup time, t_h, be expressed as:

Table 2. Derived Rate Constants

Coal Specimen	Compounds Monitored	a (1/s^ 4)	b (1/K)
Mine: River Queen Seam: Kentucky #11	Hydrocarbons (FID)	1.47×10^{-6}	9.83×10^{-3}
Mine: Powhaton Seam: Pittsburgh #8	Hydrocarbons (FID)	2.29×10^{-3}	3.34×10^{-3}
Westerholt	Hydrocarbons (FID)	5.59×10^{-6}	8.73×10^{-3}
Mine: Crown #2 Seam: Illinois #6	Hydrocarbons (FID)	6.99×10^{-8}	11.8×10^{-3}

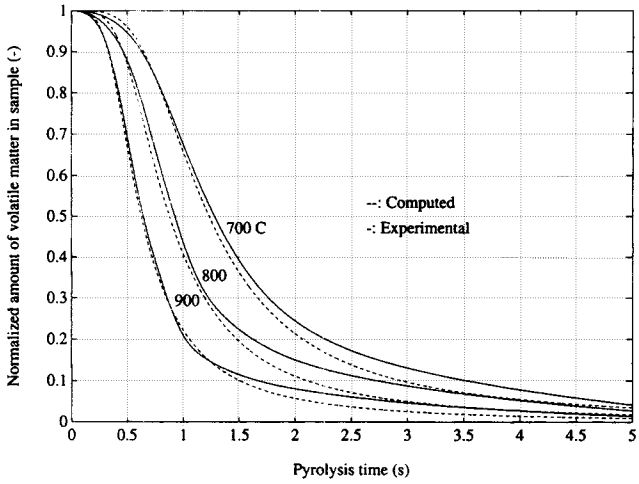

Figure 6. Experimental and computed normalized amounts of volatile matter for the Kentucky #11 coal specimen at 700, 800 and 900°C.

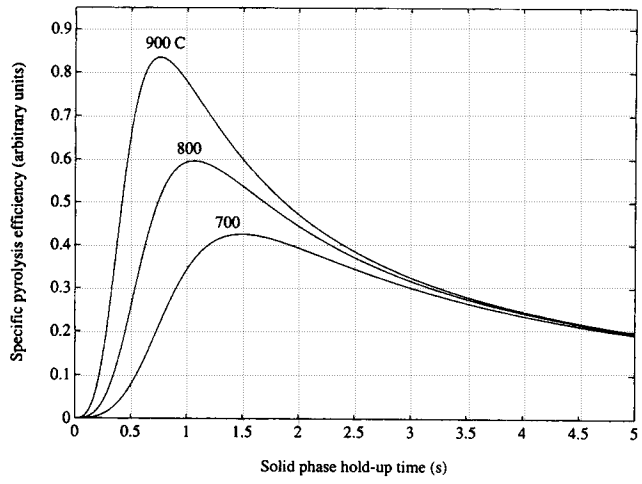

Figure 8. Experimental and computed specific pyrolysis efficiencies for the Kentucky #11 coal specimen at 700, 800 and 900°C.

$$X_{th} = 100 \cdot \left(1 - \sqrt{\frac{2}{a \exp(b\, T_{gas}) t_h^4 + 2}}\right) \tag{21}$$

Figure 7 gives X_{th} for the Kentucky #11 coal specimen using the constants in Table 2 at 700, 800 and 900°C. If assuming the heat value (ΔH) of the volatile, or more correctly the FID detectable, matter to equal that of the dry and ash free (DAF) solid matter, the pyrolysis efficiency in a continuous reactor may be quantified as a pyrolysis energy transfer power, P. With $\dot{m}$ denoting the DAF solid mass flow into the reactor, P will be given by:

$$P = \dot{m}\, \Delta H \frac{X_{th}}{100} \tag{22}$$

P may thus be expressed as a function of the reactor holdup time. The pyrolysis energy transfer power per reactor holdup time or in other words reactor size gives a specific pyrolysis efficiency, P_{eff}:

$$P_{\text{eff}} = \frac{P}{t_h} \tag{23}$$

Figure 8 gives P_{eff} in arbitrary units for the example in Figure 7. Through differentiation of Eq. 23 with respect to t_h the holdup time, t_{opt}, that maximizes P_{eff} may be derived by solving:

$$\frac{dP_{\text{eff}}}{dt_h} = 0 \tag{24}$$

Equation 24 may be solved numerically or graphically (Figure 8). The devolatilization degree at t_{opt} may be computed from Eq. 21 by substituting t_h by t_{opt}.

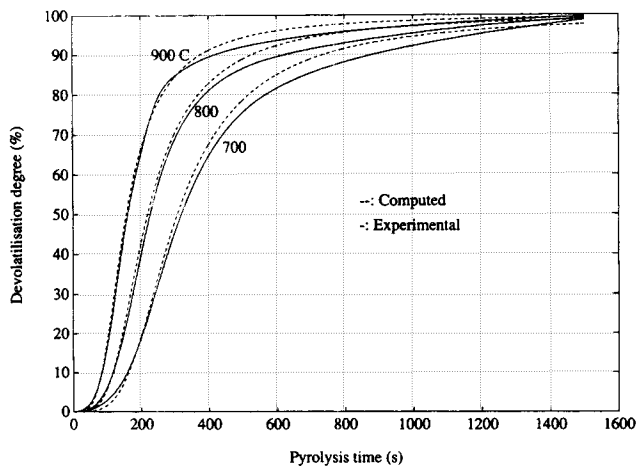

Figure 7. Experimental and computed devolatilization degrees for the Kentucky #11 coal specimen at 700, 800 and 900°C.

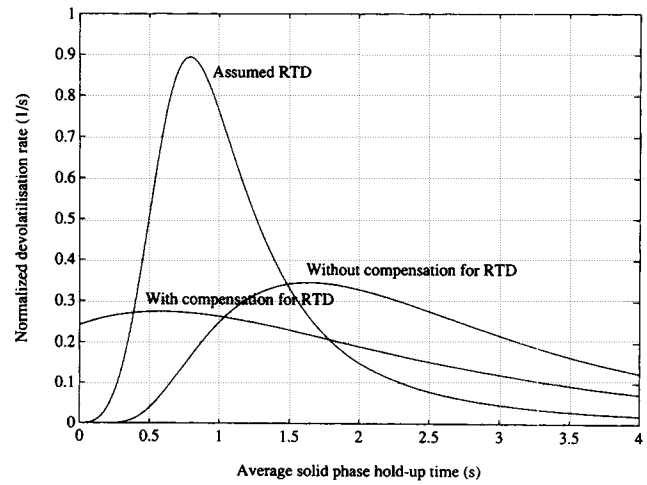

Figure 9. Normalized devolatilization rate for suggested model approach with and without compensation for an assumed RTD for Kentucky #11 coal specimen at 750°C.

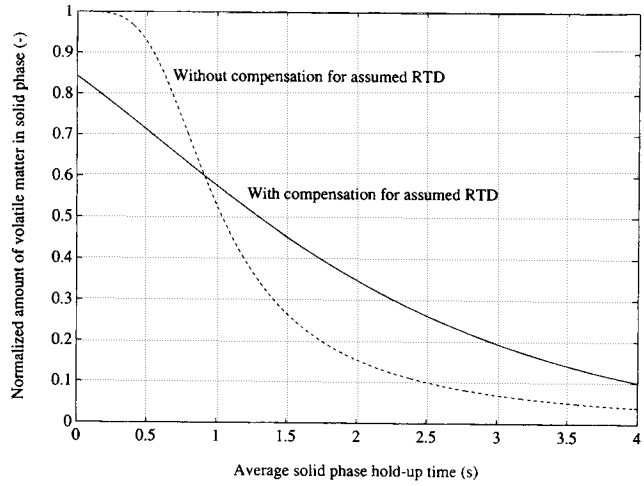

Figure 10. Devolatilization degree for suggested model approach with and without compensation for an assumed RTD for Kentucky #11 coal specimen at 750°C.

Equations 21 to 24 assume discrete reactor holdup times. In reality, though, the residence time distribution of the reactor must be compensated for. This can be done by convolving the devolatilization rate with the RTD. The RTD-compensated normalized devolatilization rate, dm'_{tRTD}/dt, will be given by:

$$\frac{dm'_{tRTD}}{dt} = \frac{dm'_t}{dt} * \text{RTD} \tag{25}$$

with * denoting the convolution operator. Equation 25 may be solved through use of Fourier transforms following:

$$\frac{dm'_{tRTD}}{dt} = F^{-1}\left[F\left[\frac{dm'_t}{dt}\right] \cdot F[\text{RTD}]\right] \tag{26}$$

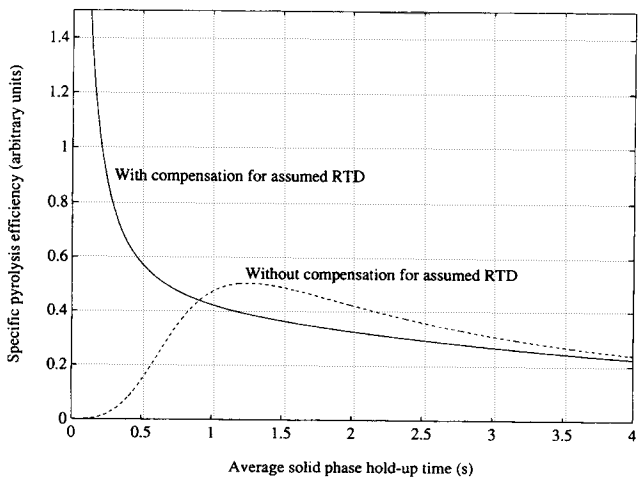

Figure 11. Specific pyrolysis efficiencies for suggested model approach with and without compensation for an assumed RTD for Kentucky #11 coal specimen at 750°C.

In doing this, the fast Fourier transform (fft) and the inverse fast Fourier transform (ifft) algorithms, with zero padding, were employed.

Figure 9 gives the normalized devolatilization rate as a function of the average holdup time for the Kentucky #11 coal at 750°C, with and without compensation for an assumed RTD. Figure 10 gives the devolatilization degree and Figure 11 the specific pyrolysis efficiency for the example in Figure 9.

If wanting to optimize the environmental performance of an energy-related pyrolysis application with respect to, for example, the sulfur emissions, the devolatilization ratio of the FID detectables over FPD detectables may be optimized for a given temperature. If X_{thCH} and X_{thS} denote the devolatilization degree of the hydrocarbons and sulfur compounds respectively. The reactor holdup time that optimizes the performance with respect to this environmental aspect be computed from:

$$\frac{d\left(\frac{X_{thCH}}{X_{thS}}\right)}{dt_h} = 0 \tag{27}$$

Equation 27 may be solved numerically or graphically as above (Figure 8). If wanting the optimum temperature with respect to this discussed environmental performance at a given holdup time, the computations are analogous, but with respect to the temperature.

Acknowledgment

Financial support from the National Energy Administration, Sweden and Asea Brown Boveri (ABB Carbon) is gratefully acknowledged.

Notation

a = rate constant in suggested model, $1/s^4$
a_1, a'_1, a_2, and a'_2 = rate constants used for developing suggested model, 1/s
b = rate constant in suggested model, 1/K
b_1 = constant used for developing suggested model, 1/K
Bi = Biot number, $= (h\,R_{eff})/K$, dimensionless
c = correlation factor in suggested model, dimensionless
C_p = heat capacity of solid, J/kg·°C
E, E_i = activation energy and activation energy for reaction i, J/mol
E_0 = mean activation energy in model assuming a Gaussian distribution of initial volatile matter amounts, J/mol
h = convective heat-transfer coefficient, J/s·°C·m^2
k_0 = Arrhenius pre-exponential factor, 1/s
k, k_i = reaction rate constant and reaction rate constant for reaction i, 1/s
K = thermal conductivity of solid, J/s·°C·m
m = mass flow of pyrolyzable matter into reactor, kg/s
m_0 = initial amount of volatile matter in sample, kg
m'_0 = normalized initial amount of volatile matter in sample, dimensionless
$m_0(k)$ = distribution of initial volatile matter amounts with respect to the reaction rate constant k, kg
m_{i0} = initial amount of volatile matter devolatilized by reaction i, kg
m_{it} = amount of volatile matter devolatilized by reaction i at time t, kg

m_t = amount of volatile matter in sample at time t, kg
m'_t = normalized amount of volatile matter in sample at time t, dimensionless
$m'_{t\text{RTD}}$ = normalized amount of volatile matter in sample after RTD compensation at average holdup time t, dimensionless
n = number of reactions included in model, dimensionless
P = energy transfer power, W
P_{eff} = specific pyrolysis efficiency, W/s
q_1 to q_i = constants in Taylor-expanded Gaussian distribution model, kg/s^{i-1}
r_{eff} = effective particle radius, m
R = universal gas constant, 8.314 J/mol/K
t = time, s
t_h = solid-phase holdup time in reactor, s
t_{opt} = solid-phase holdup time that optimizes the specific pyrolysis efficiency, s
T = absolute temperature, K
T_{gas} = gas temperature, K
T_0 = initial particle temperature, K
T_p = particle temperature, K
X_{th} = devolatilization degree at reactor holdup time t_h, %
X_{thCH} or X_{thS} = devolatilization degree of hydrocarbons or sulfur compounds at holdup time t_h, %
x = arbitrary chosen parameter, J/mol

Greek letters

ρ_p = particle density, kg/m^3
σ = standard deviation around E_0 in model assuming a Gaussian distribution of initial volatile matter amounts, J/mol

Literature Cited

Agarwal, P. K., W. E. Genetti, and Y. Y. Lee, "Model for Devolatilization of Coal Particles in Fluidized Beds," *Fuel*, **63**(8), 1157 (1984).

Anthony, D. B., J. B. Howard, H. C. Hottell, and H. P. Meissner, "Rapid Devolatilization of Pulverized Coal," *Int. Symp. on Combust.*, Combustion Institute, Pittsburgh, p. 1303 (1974).

Badzioch, S., and P. G. Hawksley, "Kinetics of Thermal Decomposition of Pulverized Coal Particles," *Ind. Eng. Chem. Process Des. Dev.*, **9**(4), 521 (1970).

Borghi, G., A. F. Sarofim,and J. M. Beér, "A Model of Coal Devolatilization and Combustion in Fluidized Beds," *Combust. and Flame*, **61**, 1 (1985).

Doolan, K. R., J. C. Mackie, M. F. R. Mulcahy, and R. J. Tyler, "Kinetics of Rapid Pyrolysis and Hydropyrolysis of a Sub-Bituminous Coal," *Int. Symp. on Combust.*, Combustion Institute, Pittsburgh, p. 1131 (1982).

Howard, J. B., "Fundamentals of Coal Pyrolysis and Hydropyrolysis," *Chemistry of Coal Utilization*, Wiley, New York (1981).

Jüntgen, H., and K. H. van Heek, "Reaktionsabläufe unter nicht isothermen Bedingungen," *Fortschritte der Chemischen Forschung*, **13**(3-4), 601 (1970).

Jüntgen, H., "Review of the Kinetics of Pyrolysis and Hydropyrolysis in Relation to the Chemical Constitution of Coal," *Fuel*, **63**(6), 731 (1984).

Kobayashi, H., J. B. Howard, and A. F. Sarofim, "Coal Devolatilization at High Temperature," *Int. Symp. on Combust.*, Combustion Institute, Pittsburgh, p. 411 (1977).

Liliedahl, T., K. Sjöström, and L-P. Wiktorsson, "Analysis Method of Pyrolysis Kinetics Using Modern Signal Processing Techniques," *AIChE J.*, **37**(9), 1415 (1991).

Niksa, S., W. B. Russel, and D. A. Saville, "Time-Resolved Weight Loss Kinetics for the Rapid Devolatilization of a Bituminous Coal," *Int. Symp. on Combus.*, Combustion Institute, Pittsburgh, p. 1139 (1982).

Niksa, S., "Modeling the Devolatilization Behaviour of High Volatile Bituminous Coals," *Int. Symp. on Combust.*, Combustion Institute, Pittsburgh, p. 105 (1988).

Nilsson, T., "Modeling of Gasification in a Fluidized Bed," ScD Thesis, Kungl Tekniska Högskolan, Stockholm (1990).

Pitt, G. J., "The Kinetics of the Evolution of Volatile Products from Coal," *Fuel*, **41**, 267 (1962).

Pyle, D. L., and C. A. Zaror, "Heat Transfer and Kinetics in the Low Temperature Pyrolysis of Solids," *Chem. Eng. Sci.*, **39**(1), 147 (1984).

Reuther, J. J., R. D. Daley, J. J. Warchol, and J. A. Withum, "Coal Volatiles—Coal Pyrolysis Analogy, Observation of 'Low' Apparent Global Activation Energies," *Fuel*, **63**(5), 604 (1984).

Saito, M., M. Sadakata, M. Sato, and T. Sakai, "Devolatilization Characteristics of Single Coal Particles for Combustion in Air and Pyrolysis in Nitrogen," *Fuel*, **66**, 717 (1987).

Solomon, P. R., and M. B. Colkert, "Coal Devolatilization," *Int. Symp. on Combust.*, Combustion Institute, Pittsburgh, p. 131 (1979).

Solomon, P. R., D. G. Hamblen, R. M. Carangelo, and J. L. Krause, "Coal Thermal Decomposition in an Entrained Flow Reactor: Experiments and Theory," *Int. Symp. on Combust.*, Combustion Institute, Pittsburgh, p. 1139 (1982).

Solomon, P. R., and D. G. Hamblen, "Finding Order in Pyrolysis Kinetics," *Prog. Energy Combust. Sci.*, **9**(4), 323 (1983).

Solomon, P. R., M. A. Serio, R. M. Carangelo, and J. R. Markham, "Very Rapid Coal Pyrolysis," *Fuel*, **65**(2), 182 (1986).

Suuberg, E. M., W. A. Peters, and J. B. Howard, "Product Composition and Kinetics of Lignite Pyrolysis," *Ind. Eng. Chem. Process Des. Dev.*, **17**(1), 37 (1978).

Manuscript received Feb. 22, 1993, and revision received Aug. 18, 1993.